Dielectric response in insulators: A wave-vector- and frequency-dependent model

J.J.M. Michiels
Research Institute for Materials, University of Nijmegen, Toernooiveld, NL-6525 ED Nijmegen, The Netherlands

L. Hedin
Department of Theoretical Physics, University of Lund, Sölvegatan 14A, S-223 62 Lund, Sweden

J.E. Inglesfield
Research Institute for Materials, University of Nijmegen, Toernooiveld, NL-6525 ED Nijmegen, The Netherlands

(Received 29 April 1994; revised manuscript received 6 July 1994)

We have calculated a random-phase-approximation-type expression for the dielectric-response function of several large-band-gap insulators using a development of the model suggested by Fry. This model should be good for systems with well-localized valence-electron functions and flat valence-electron bands. We show that in this model it is a minor approximation to use spherically symmetric bands in the integration over reciprocal space. This allows simple and fast evaluations of our expressions, thus avoiding Brillouin-zone integrations and summations over band indices. The results of our calculations are compared with *ab initio* data on static dielectric matrices from Baldereschi and Tosatti, with model calculations on the static dielectric function from Rezvani and Friauf, and with electron-energy-loss spectra for LiF from Fields *et al.*, using only one fit parameter. In addition, the Johnson f-sum rule is tested for this model. We also verify that our approximation gives the correct singular behavior of the $(0, \mathbf{K})$ matrix elements.

I. INTRODUCTION

In this paper we present a model for the wave-vector- and frequency-dependent dielectric function applicable to insulators such as NaCl, MgO, and LiF. They are all characterized by relatively flat valence bands and a conduction band which is more free-electron-like. We shall show that a dielectric function using a simple model of this electronic structure can reproduce quite successfully the response of the system to perturbations with varying wave vector and frequency, including local field effects. Calculations of the dielectric function (usually within the random-phase approximation) based on *ab initio* electronic structure calculations[1] require a large computational effort and for this reason model dielectric functions are useful. This is particularly so when the dielectric function is used to calculate the screened interaction between electrons in self-energy calculations.[2–4] Moreover, model calculations can bring out the physical aspects of the dielectric response.

Most of these calculations give an analytically tractable function for describing the dynamical response. In particular, in self-energy calculations these dielectric functions lead to simple expressions for the self-energy operator.[4] Usually, these models involve a one-oscillator approximation in which the valence and conduction bands are assumed to be completely flat and the oscillator strength is determined by sum rules.[5,6] For some applications, such as self-energy calculations, or simulation of electron-energy-loss spectra (EELS), a more detailed description of dynamical response may be required. Also, it is not clear from these simple models how the spatial extent of the wave functions affects the dielectric response and subsequently the self-energy corrections. Other existing models, such as those of Hanke and Sham,[7] and Inkson and Turner,[8] can meet these requirements but they involve considerable computation when the dielectric function has to be evaluated at various frequencies and wave vectors including local fields. These models present the dielectric function in the Wannier representation and involve a band-structure interpolation. Concluding, there is clearly room for improvement in the choice of model dielectric functions for large-band-gap insulators in which the dispersive conduction band makes the one-oscillator model inapplicable, particularly if we wish to avoid the involved calculations of the second class of models.

The model described in this paper is a development of the model suggested by Fry.[9] This represents the valence states by tight-binding Bloch states and the conduction states by plane waves orthogonalized to the valence states; the band structure of the unoccupied states is modeled by free-electron-like (parabolic) bands. The dielectric function calculated in this way has been applied by Rezvani and Friauf to several large-band-gap insulators.[10] We extend the model dielectric function by including the conduction band density of states from a self-consistent band-structure calculation and local field effects, and derive analytic simplifications. This model provides both an accurate and simple expression for the dielectric function of a wide class of compounds contain-

ing only the spatial extent of the valence states as a parameter. In Sec. II we evaluate the model dielectric function, keeping in mind the analytic requirements of such a function. Details of this evaluation are moved to the appendices. In Sec. III the model results will be presented and tested by comparing them to the zero-frequency model and *ab initio* results for a number of systems (MgO, KCl, Ar, NaCl), to experimental results (wave-vector- and frequency-dependent EELS spectra of LiF) and by checking f-sum rule conditions. These results will be discussed and related to the particular choice of the model formulation. Concluding remarks are then given in Sec. IV. We will use atomic units throughout, with $e = \hbar = m = 1$, and the unit of energy is the Hartree =27.2 eV.

II. THEORY

The longitudinal dielectric function ϵ relates in linear response the induced potential to the total change in potential. In a plane wave representation we have

$$\delta\phi_{\rm ind}(\mathbf{q},\mathbf{K},\omega) = \sum_{\mathbf{K}'} G_{\mathbf{K},\mathbf{K}'}(\mathbf{q},\omega)\delta\phi_{\rm tot}(\mathbf{q},\mathbf{K}',\omega) \ , \quad (1)$$

where

$$G_{\mathbf{K},\mathbf{K}'}(\mathbf{q},\omega) = \delta_{\mathbf{K},\mathbf{K}'} - \epsilon_{\mathbf{K},\mathbf{K}'}(\mathbf{q},\omega) \quad (2)$$

and $\mathbf{K}$ and $\mathbf{K}'$ are reciprocal lattice vectors. $\delta\phi_{\rm tot}(\mathbf{q},\mathbf{K}',\omega)$ is a frequency- (ω) and wave-vector- ($\mathbf{q}+\mathbf{K}'$) dependent potential, which consists of a slowly varying contribution due to the external charge perturbation plus the induced potential. In the random-phase approximation the function $G_{\mathbf{K},\mathbf{K}'}(\mathbf{q},\omega)$ is evaluated starting from one-electron wave functions and energies obtained from a density functional band-structure calculation, and perturbation theory then gives[11]

$$\epsilon_{\mathbf{K},\mathbf{K}'}(\mathbf{q},\omega) = \delta_{\mathbf{K},\mathbf{K}'} - \frac{2\times 4\pi}{|\mathbf{q}+\mathbf{K}|^2\Omega}\sum_{\mathbf{k},l,l'}\frac{f_0(E_{\mathbf{k}+\mathbf{q},l'}) - f_0(E_{\mathbf{k},l})}{E_{\mathbf{k}+\mathbf{q},l'} - E_{\mathbf{k},l} - \omega - i0^+}$$
$$\times\langle\mathbf{k},l|e^{-i(\mathbf{q}+\mathbf{K})\cdot\mathbf{r}}|\mathbf{k}+\mathbf{q},l'\rangle\langle\mathbf{k}+\mathbf{q},l'|e^{i(\mathbf{q}+\mathbf{K}')\cdot\mathbf{r}}|\mathbf{k},l\rangle, \quad (3)$$

where the matrix elements are taken between single-particle Bloch states of wave vectors $\mathbf{k}, \mathbf{k}+\mathbf{q}$ and band indices l, l'.

In this section we shall derive a computationally convenient form for ϵ based on (3) for the class of insulators with a relatively flat valence band and a much more dispersive conduction band. This class includes ionic solids like LiF, MgO, NaCl, and the noble gas solids. Figure 1 shows the band structure of LiF, for example.[12] This form of band structure makes a one-oscillator form for ϵ, such as suggested in the work of Johnson[5] and Ortuna and Inkson,[6] unsuitable. The one-oscillator model assumes that the dielectric reponse is dominated by one particular transition and that the contributions from the other part of the excitation spectrum can be neglected. For the class of compounds we consider here this is not the case.

We therefore require a form of dielectric function in which the model wave functions and energy bands reflect the properties of these compounds. For the valence states, which are very localized and have predominantly p character, we choose tight-binding Bloch states using $2p$ atomic orbitals as localized wave functions on the anion sites:

$$|\mathbf{k}_\mu\rangle = \frac{1}{\sqrt{N}}\sum_j p_\mu(\mathbf{r}-\mathbf{R}_j)e^{i\mathbf{k}\cdot\mathbf{R}_j}, \quad (4)$$

where the form of the atomic functions is taken from Ref. 13:

$$p_\mu(\mathbf{r}) = \frac{1}{\pi}\sum_\nu c_\nu\lambda_\nu^{\frac{5}{2}} r e^{-\lambda_\nu r}\Phi_\mu(\phi,\theta). \quad (5)$$

The angular function represents the angular part of the $2p_x$, $2p_y$, and $2p_z$ functions [$\mu = x$, y, or z; the particular choice of the atomic orbitals is related to the particular type of lattice being considered here (face-centered cubic)]. The choice of this type of function agrees with the pseudopotential picture[14] of large-band-gap insulators in which valence wave functions have mainly p character without radial nodes in the atomic region. Turning to the unoccupied states we represent the wave functions as plane waves which are orthogonalized to the valence states:

$$|\mathbf{k},l\rangle = a_{\mathbf{k},l}\left(|\mathrm{PW}_{\mathbf{k},l}\rangle - \sum_\mu\langle\mathbf{k}_\mu|\mathrm{PW}_{\mathbf{k},l}\rangle|\mathbf{k}_\mu\rangle\right) \ , \quad (6)$$

where

$$|\mathrm{PW}_{\mathbf{k},l}\rangle = \frac{1}{\sqrt{\Omega}}e^{i(\mathbf{k}+\mathbf{Q}_l)\cdot\mathbf{r}}, \quad (7)$$

$a_{\mathbf{k},l}$ is the normalization factor, and $\mathbf{Q}_l$ is the reciprocal lattice vector which translates the free-electron band back into band l within the first Brillouin zone. This representation of valence and conduction band states, which was suggested by Fry,[9] will lead to an analytic expression for ϵ. As we shall see, this expression will have the correct analytical behaviour at $\mathbf{q}\to\mathbf{0}$, which is required for elements of the dielectric matrix.

When we neglect the dispersion of the valence states and set their energy equal to a constant E_v—this is a good approximation for large-band-gap insulators—we arrive at

$$\mathrm{Im}\epsilon_{\mathbf{K},\mathbf{K}'}(\mathbf{q},\omega) = \frac{1}{|\mathbf{q}+\mathbf{K}|^2\Omega_0\pi}\sum_{\mu}\int d^3\kappa a_\kappa^2\delta(E(\kappa)-E_v-\omega) \times F_\mu(\kappa,\mathbf{q},\mathbf{K})F_\mu^*(\kappa,\mathbf{q},\mathbf{K}'), \tag{8}$$

where

$$F_\mu(\kappa,\mathbf{q},\mathbf{K}) = \int d^3r p_\mu(\mathbf{r})e^{i[\kappa-(\mathbf{q}+\mathbf{K})]\cdot\mathbf{r}} - \int d^3r p_\mu^2(\mathbf{r})e^{-i(\mathbf{q}+\mathbf{K})\cdot\mathbf{r}} \times \int d^3r p_\mu(\mathbf{r})e^{i\kappa\cdot\mathbf{r}}. \tag{9}$$

This is the expression at positive frequency ω. The real part can be evaluated from (8) by a Kramers-Kronig principal value integral. In the above expression we ignore the overlap of p functions on separate atoms, which actually corresponds to having no dispersion, and contributions from integrals like $\int d^3r p_\mu(\mathbf{r})p_\nu(\mathbf{r})e^{-i(\mathbf{q}+\mathbf{K})\cdot\mathbf{r}}$, which is a good approximation for systems with localized valence functions. For these systems the normalization constant a_κ is close to unity and slowly varying with κ—this has been tested in numerical calculations where deviations from unity were generally smaller than 2%—and therefore we put $a_\kappa = 1.0$ in the following expressions. The integrals of p and p^2 functions in (9) are evaluated in Appendix A. The integration with respect to κ in (8) is over all of reciprocal space. Ω_0 is the volume of the primitive unit cell. The summation over μ indicates the contribution to $\epsilon_{\mathbf{K},\mathbf{K}'}(\mathbf{q},\omega)$ of the $2p_x$, $2p_y$, and $2p_z$ functions.

The κ integration can be greatly simplified because of the rather slow variation of F_μ with $|\kappa|$. The δ function in (8) picks out a constant energy surface, which as far as F_μ is concerned can be replaced by a spherical surface of the same area. The radial integration in (8) gives a density of states factor, which appears outside the angular integral. The final expression for the dielectric function is then

$$\mathrm{Im}\epsilon_{\mathbf{K},\mathbf{K}'}(\mathbf{q},\omega) = \frac{\pi g(E_v+\omega)}{|\mathbf{q}+\mathbf{K}|^2\Omega_0}\sum_{\mu}\int d\theta_\kappa \sin\theta_\kappa \int d\phi_\kappa [F_\mu(\kappa,\mathbf{q},\mathbf{K})F_\mu^*(\kappa,\mathbf{q},\mathbf{K}')]_{\kappa^2=2m^*(\kappa)(E_v+\omega)}, \tag{10}$$

where $g(E_v+\omega)$ is the total density of unoccupied states per unit volume and where the constraint condition $\kappa^2 = 2m^*(\kappa)(E_v+\omega)$ arises from the radial integration. This condition, in which $m^*(\kappa)$ is the effective mass corresponding to the spherical energy surface, can be approximated by a simpler one in which m^* is a constant. This is also due to the rather slow variation of F_μ with $|\kappa|$. The angular integration is a measure of the oscillator strength, and determines the analytical properties of $\epsilon_{\mathbf{K},\mathbf{K}'}(\mathbf{q},\omega)$. The analytic evaluation of this integral is very involved and we have moved details of the calculation to Appendix B.

In the following we will first consider the required analytical properties for the elements of the dielectric matrix in (3). In particular the head and body of the dielectric matrix, which contain, respectively, the elements $\epsilon_{0,0}(\mathbf{q},\omega)$ and $\epsilon_{\mathbf{K},\mathbf{K}'}(\mathbf{q},\omega)$ ($\mathbf{K},\mathbf{K}'$ are nonzero vectors) are analytic functions for $\mathbf{q}\to\mathbf{0}$, while the remaining elements (which build the "wings" of the matrix) are nonanalytic under these conditions. These requirements have been discussed in earlier papers[15] for the dielectric matrix elements in (3), but it is not immediately obvious that the model being discussed here fulfils these conditions.

For $\mathbf{K},\mathbf{K}'$ nonzero, ϵ is indeed an analytic function. However, when $\mathbf{K}$ or $\mathbf{K}'$ equals $\mathbf{0}$ and $\mathbf{q}\to\mathbf{0}$ the situation is different. Then

$$F_\mu(\kappa,\mathbf{q},0) = -\mathbf{q}\cdot\nabla_{\mathbf{Q}}\int d^3r p_\mu(\mathbf{r})e^{i\mathbf{Q}\cdot\mathbf{r}}\Big|_{\mathbf{Q}=\kappa} + O(q^2), \tag{11}$$

and for $\mathbf{q}\to\mathbf{0}$ we have $F_\mu(\kappa,\mathbf{q},0) = -F_\mu(\kappa,-\mathbf{q},0)$. Consequently, for the symmetrical dielectric matrix, which is defined as

$$\bar{\epsilon}_{\mathbf{K},\mathbf{K}'}(\mathbf{q},\omega) = \frac{|\mathbf{q}+\mathbf{K}|}{|\mathbf{q}+\mathbf{K}'|}\epsilon_{\mathbf{K},\mathbf{K}'}(\mathbf{q},\omega), \tag{12}$$

the relation $\bar{\epsilon}_{\mathbf{K},0}(\mathbf{q},\omega) = -\bar{\epsilon}_{\mathbf{K},0}(-\mathbf{q},\omega)$ follows. However, the function does not vanish as $\mathbf{q}\to\mathbf{0}$ which by definition means the function is nonanalytic at $\mathbf{q}=\mathbf{0}$. In this case a separate prescription is needed and this can be provided by gauge invariance which requires no electronic response to a constant potential. Therefore the matrix elements of the wings are equal to zero at $\mathbf{q}=\mathbf{0}$. When both vectors $\mathbf{K}$ and $\mathbf{K}'$ are equal to zero these problems do not occur. The prefactor $1/|\mathbf{q}+\mathbf{K}|^2$ in (10) is cancelled by the product of F_μ functions in the angular integration and this results in a finite value for $\epsilon_{0,0}(\mathbf{q},\omega)$ which is independent of the direction of $\mathbf{q}$ when $\mathbf{q}\to\mathbf{0}$. Therefore the head of the matrix is an analytic function. This completes the arguments that the model dielectric function has the desired analytic properties. We have already mentioned that the orthogonalization of conduction band states to the valence states is necessary for the required analytic behavior. This can be understood from a consideration of F_μ in (9) and (11) with which the analytic properties of the matrix elements were explained. The function F_μ has two contributions which cancel one another as $\mathbf{q}\to\mathbf{0}$, as shown in (9) and (11), where the first contribution is due to the plane wave term in (6) and the second one comes from the mixing of the plane wave with the valence wave function of equivalent crystal momentum.

The analytic evaluation of (10) has been tested by numerical calculations and all summation cutoffs (see Appendix B) have been chosen so that the results are con-

verged to within 1%. In the angular integration in (10) the number of radial basis functions for the $2p$ wave functions is limited to 1, which means there is only one fit parameter. The value of the band gap is fixed by the particular application. For example, in comparisons of model results with *ab initio* data the band gap will be set equal to the band gap from this *ab initio* calculation, and in applications to optical spectra the optical band gap will be used.

In order to illustrate that the model dielectric function has a reasonable form for its frequency dependence for systems with a band gap, in Fig. 2 we compare this model with *ab initio* data for Si.[4] For the purpose of this shape comparison the model results were calculated with the band gap and atomic volume appropriate to Si. We do not claim perfect agreement in this case, because for the unoccupied states the free-electron density of states is used as input. Moreover, the model is not really designed to describe systems with significant dispersion in the valence band. In Fig. 2 also the effect of varying the exponential parameter, which describes the extent of the

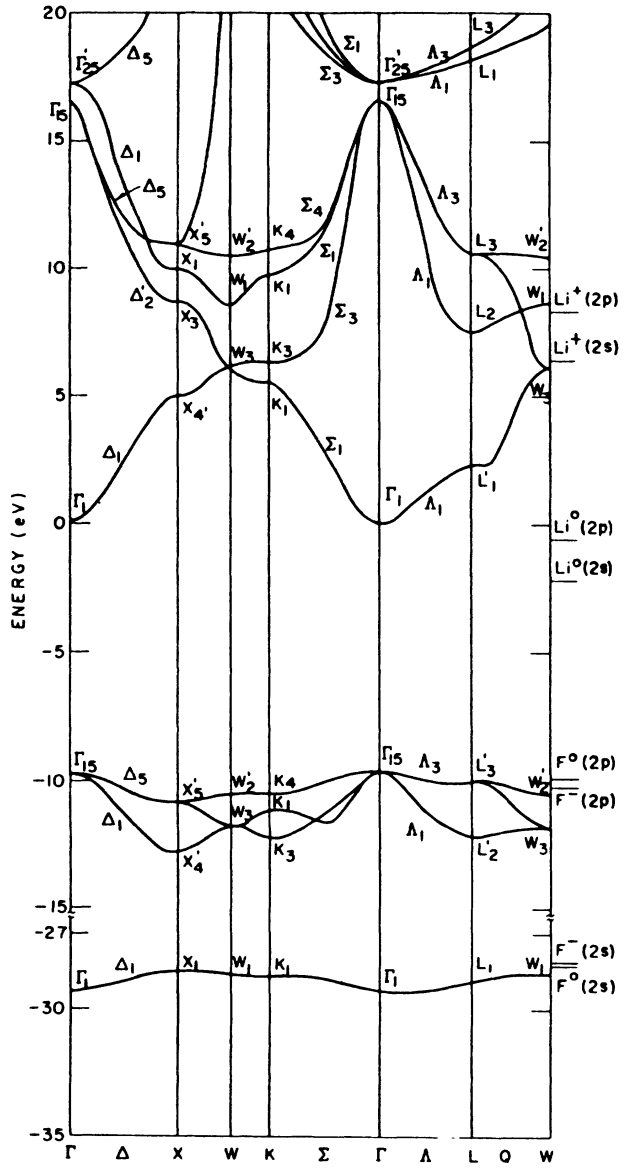

FIG. 1. Self-consistent band structure of LiF (Ref. 12) in the $\alpha = 2/3$ exchange model.

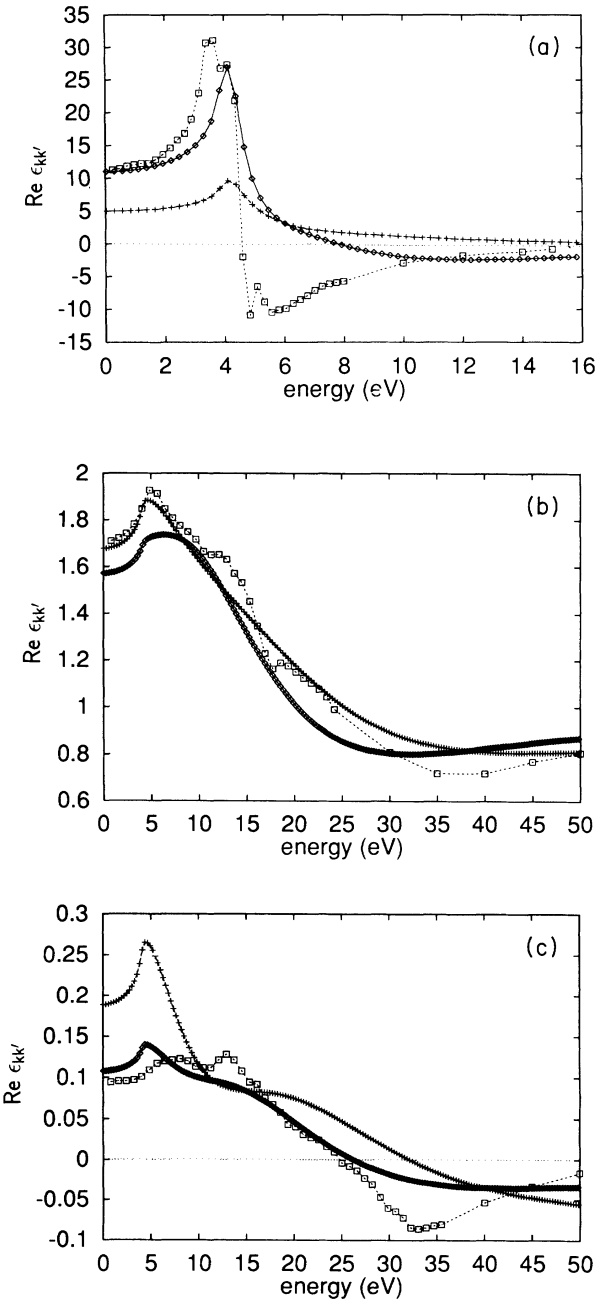

FIG. 2. The dependence of $\mathrm{Re}\epsilon_{\mathbf{K},\mathbf{K}'}(0,\omega)$ as a function of ω for a number of combinations of $\mathbf{K}$ and $\mathbf{K}'$. The lattice parameter is 10.26 a.u., and the band gap is taken to be 4.0 eV. The exponential parameters are λ=0.72 a.u.$^{-1}$ (diamonds) and λ=1.00 a.u.$^{-1}$ (crosses). In the model calculation a free-electron density of states is used. In (a), (b), and (c) the combinations of $\mathbf{K}$ and $\mathbf{K}'$ are, respectively, {(000),(000)}, {(111),(111)}, and {(111),(200)}. For comparison the *ab initio* results for silicon from Ref. 4 are presented (squares).

valence wave function, is illustrated. The results are consistent with the physical notion that in a more localized charge distribution [large λ in (5)], where the electrons are more tightly bound to the ion cores, the dielectric response to external charge disturbances is reduced.

III. RESULTS AND DISCUSSION

In this section we present data which will show that the model dielectric function gives an accurate description of dielectric response in large-band-gap insulators. For this purpose several comparisons of model results with *ab initio* data and experimental results have been made. These involve calculations of dielectric matrices at $\omega = 0$ and $\mathbf{q} \to \mathbf{0}$ and simulations of electron-energy-loss spectra. We will start, however, with a comparison of our results with model results from Rezvani and Friauf,[10] who apply Fry's model[9] to calculating $\epsilon_{0,0}(\mathbf{q},\omega)$ for several large-band-gap systems (Ar and KCl). Their model has a similar representation of the valence and conduction band states, which are, respectively, tight-binding wave functions and plane waves orthogonalized to the valence states, but it treats the band structure in a different manner from ours. The valence states have some dispersion, and the conduction bands are represented by a small number of parabolic bands in the reduced zone scheme. Another difference in Rezvani and Friauf's model is the numerical evaluation of the sum in (3), using the spherical zone approximation, whereas we treat this analytically in (10). We can expect to obtain very similar results, however, by using a free-electron density of states with the same effective mass as in their calculations. This is indeed the case. For Ar they obtained $\epsilon_{0,0}(0,0) = 1.70$ for $\lambda = 1.18$ a.u.$^{-1}$. We find $\epsilon_{0,0}(0,0) = 1.70$ for $\lambda = 1.16$ a.u.$^{-1}$. For KCl there is also excellent agreement: they obtained $\epsilon_{0,0}(0,0) = 2.13$ for $\lambda = 0.84$ a.u.$^{-1}$, while our calculations show that $\epsilon_{0,0}(0,0) = 2.13$ for $\lambda = 0.89$ a.u.$^{-1}$. The small differences are probably due to the fact that in Rezvani and Friauf's calculation only two parabolic bands were taken into account, whereas in our model calculation the free-electron band structure up to 60 eV above the bottom of the conduction band was considered.

Additional support for our model dielectric function comes from the comparison of the symmetric dielectric matrices with the *ab initio* results of Baldereschi and Tosatti[15] for the particular case of $\omega = 0$ and $\mathbf{q} \to \mathbf{0}$ [$\mathbf{q}\|(100)$]. In the model calculations the matrices are obtained for a particular value of λ in (5) which is obtained by fitting the $(0,0)$ element of $\epsilon_{\mathbf{K},\mathbf{K}'}(\mathbf{q},0)$ to the *ab initio* value. In Tables I and II the results of two of these calculations, for MgO and NaCl, are given with the free-electron density of states as input. The radial function exponents λ are, respectively, 1.10 a.u.$^{-1}$ and 0.91 a.u.$^{-1}$. In order to achieve better agreement in the case of NaCl we also introduce the density of unoccupied states from a band-structure calculation, using the LSW (localized spherical wave) approach.[16] These results are given in Table III and the agreement between model and *ab initio* results is excellent except at larger reciprocal

TABLE I. Matrix elements of the symmetric dielectric matrix $\bar{\epsilon}$ for MgO, $\mathbf{q}\|(100)$ and $\mathbf{q} \to \mathbf{0}$. The *ab initio* results are from Baldereschi and Tosatti (Ref. 15). The free-electron density of states is used as input.

$\mathbf{K}$	$\mathbf{K}'$	$\bar{\epsilon}_{\mathbf{K},\mathbf{K}'}(\mathbf{q},\omega=0)$ *ab initio*	$\bar{\epsilon}_{\mathbf{K},\mathbf{K}'}(\mathbf{q},\omega=0)$ model
(000)	(000)	3.180	3.180
(111)	(000)	-0.325	-0.293
(111)	(111)	1.430	1.179
($\bar{1}$11)	(111)	0.081	0.030
(1$\bar{1}$1)	($\bar{1}$11)	-0.041	-0.004
(1$\bar{1}\bar{1}$)	($\bar{1}$11)	-0.131	-0.014
(200)	(200)	1.298	1.399
(200)	($\bar{1}$11)	0.029	0.044
(200)	(111)	-0.107	-0.075
(200)	(000)	0.342	0.328
(200)	($\bar{2}$00)	-0.055	0.381
(020)	(200)	0.002	-0.170

TABLE II. Matrix elements of the symmetric dielectric matrix $\bar{\epsilon}$ for NaCl, $\mathbf{q}\|(100)$ and $\mathbf{q} \to \mathbf{0}$. The *ab initio* results are from Baldereschi and Tosatti (Ref. 15). The free-electron density of states is used as input.

$\mathbf{K}$	$\mathbf{K}'$	$\bar{\epsilon}_{\mathbf{K},\mathbf{K}'}(\mathbf{q},\omega=0)$ *ab initio*	$\bar{\epsilon}_{\mathbf{K},\mathbf{K}'}(\mathbf{q},\omega=0)$ model
(000)	(000)	2.514	2.517
(111)	(000)	-0.330	-0.182
(111)	(111)	1.470	1.207
($\bar{1}$11)	(111)	0.091	0.000
(1$\bar{1}$1)	($\bar{1}$11)	-0.052	0.000
(1$\bar{1}\bar{1}$)	($\bar{1}$11)	-0.182	0.000
(200)	(200)	1.347	1.397
(200)	($\bar{1}$11)	0.062	-0.036
(200)	(111)	-0.143	-0.069
(200)	(000)	0.407	0.001
(200)	($\bar{2}$00)	-0.090	-0.357
(020)	(200)	0.005	0.004

TABLE III. Matrix elements of the symmetric dielectric matrix $\bar{\epsilon}$ for NaCl, $\mathbf{q}\|(100)$ and $\mathbf{q} \to \mathbf{0}$. The *ab initio* results are from Baldereschi and Tosatti (Ref. 15). The calculated density of states is used as input. See text.

$\mathbf{K}$	$\mathbf{K}'$	$\bar{\epsilon}_{\mathbf{K},\mathbf{K}'}(\mathbf{q},\omega=0)$ *ab initio*	$\bar{\epsilon}_{\mathbf{K},\mathbf{K}'}(\mathbf{q},\omega=0)$ model
(000)	(000)	2.514	2.511
(111)	(000)	-0.330	-0.336
(111)	(111)	1.470	1.420
($\bar{1}$11)	(111)	0.091	0.096
(1$\bar{1}$1)	($\bar{1}$11)	-0.052	-0.031
(1$\bar{1}\bar{1}$)	($\bar{1}$11)	-0.182	-0.082
(200)	(200)	1.347	1.782
(200)	($\bar{1}$11)	0.062	0.039
(200)	(111)	-0.143	-0.143
(200)	(000)	0.407	0.422
(200)	($\bar{2}$00)	-0.090	0.475
(020)	(200)	0.005	-0.237

lattice vectors. Here $\lambda = 1.255$ a.u.$^{-1}$ and the effective mass parameter $m^* = 1.31$.

A further test for the model dielectric function is provided by the f-sum rule due to Johnson,[5] which is applicable to the RPA dielectric function:

$$\int_0^\infty d\omega\omega \mathrm{Im}\epsilon_{\mathbf{K},\mathbf{K}'}(\mathbf{q},\omega) = -\tfrac{1}{2}\pi\omega_p^2 f(\mathbf{K}-\mathbf{K}')\hat{\mathbf{e}}(\mathbf{q}+\mathbf{K})\cdot\hat{\mathbf{e}}(\mathbf{q}+\mathbf{K}'). \quad (13)$$

$\hat{\mathbf{e}}$ is a unit vector which has the direction of its argument and $f(\mathbf{K})$ represents the Fourier transform of the charge density. It provides a good test of our approach for including the effects of band structure and oscillator strength in the dielectric function. We have checked the sum rule equation for the model dielectric function, using the NaCl parameters and the calculated density of unoccupied states. The results, which are given in Table IV give a very convincing statement of the accuracy of the model dielectric function.

Another demonstration is provided by a simulation of the electron-energy-loss spectra for LiF.[17] These spectra are measurements of the partial differential cross section $\frac{\partial^2\sigma}{\partial\Omega\partial E}$, which gives the fraction of incident electrons with primary energy E_0 scattered into solid angle $d\Omega$ and energy between E_1 and $E_1 + dE$ when traversing the solid.[18] This quantity is proportional to $\mathrm{Im}\epsilon_{0,0}^{-1}(\mathbf{q},\omega)$, where $\mathbf{q}$ is the momentum transfer and ω is the energy loss $(E_0 - E_1)$. We compare in Fig. 3 the experimental electron-energy-loss spectra as a function of energy, and for several directions and magnitudes of the momentum transfer, with corresponding model results for $\mathrm{Im}1/\epsilon_{0,0}(\mathbf{q},\omega)$ in which local field effects have been neglected for the moment. In our calculations we include the unoccupied density of states of LiF, which was calculated up to approximately 60 eV above the Fermi energy, using the LSW approach[16] with an extended basis set. The effective mass parameter in (10) is set equal to 1.0 and this is in agreement with the dispersion of the lowest conduction band in the band structure. In order to determine λ in (5), $\mathrm{Im}1/\epsilon_{0,0}(\mathbf{q},\omega)$ is fitted to the experimental spectrum for $q = 0.23$ a.u.$^{-1}$ and $\mathbf{q}\|(100)$. This gives $\lambda = 1.80$ a.u.$^{-1}$ and with this parameter also the other $\Im\mathrm{m}1/\epsilon_{0,0}(\mathbf{q},\omega)$ curves as a function of energy ω have been obtained. In all cases the agreement between experimental and calculated spectral shape is excellent, except for the region just above the band gap, up to 10 eV above the band gap. This energy range is dominated by an exciton structure, which cannot be treated within a density functional band-structure calculation. At larger values of the momentum transfer the exciton structure decreases [see, for example, Fig. 3(c) and 3(f)] and the agreement between experimental and theoretical spectra is therefore improved. This may indicate a relation between momentum transfer and the strength of the electron-hole interaction. Finally we note the splitting in the experimental plasmon peak at 25 eV for larger q, which is not reproduced in the calculated spectra. This is possibly related to our assumption of a flat valence band, whereas in the case of LiF the valence bandwidth is 3.5 eV,[19] consistent with the plasmon peak splitting.

Up to this point we have not included local field corrections in the macroscopic dielectric response. These local fields are rapidly varying charge fluctuations of wave vector $\mathbf{q}+\mathbf{K}$ produced by an external perturbation of wave vector $\mathbf{q}$, where $\mathbf{q}$ is generally much smaller than the shortest reciprocal lattice vector $\mathbf{K}$. In order to include these local fields into a description of dielectric response a matrix representation for the dielectric function, e.g., (3), is required,[11] in which the off-diagonal terms represent the local fields. The effect of these local fields on macroscopically important phenomena, such as the energy loss of fast electrons and the absorption of radiation in solids, can be understood from the relation between

TABLE IV. Test of the sum rule condition in (13) for our model dielectric function. This is done for a number of $\mathbf{q}$, $\mathbf{K}$, $\mathbf{K}'$ combinations, using the NaCl parameters and calculated density of states. The magnitude of wave vector $\mathbf{q}$ is given in a.u.$^{-1}$.

K	K′	q	lhs of (13)	rhs of (13)
(000)	(000)	0.10, ‖ (100)	-0.259	-0.249
(000)	(000)	0.30, ‖ (100)	-0.279	-0.249
(000)	(000)	1.18, ‖ (100)	-0.241	-0.249
K	**K′**	**q**	lhs of (13)	rhs of (13)
(000)	(000)	0.10, ‖ (111)	-0.255	-0.249
(000)	(000)	0.30, ‖ (111)	-0.241	-0.249
(000)	(000)	0.50, ‖ (111)	-0.218	-0.249
K	**K′**	**q**	lhs of (13)	rhs of (13)
(200)	(111)	0.00	-0.047	-0.065
$(\bar{1}11)$	(111)	0.00	-0.026	-0.029
(111)	$(\bar{1}\bar{1}\bar{1})$	0.00	0.024	0.011

the dielectric matrix in (3) and the macroscopic dielectric function[11]

$$\epsilon_M(\mathbf{q},\omega) = \frac{1}{\epsilon^{-1}_{0,0}(\mathbf{q},\omega)}. \tag{14}$$

$\epsilon_M(\mathbf{q},\omega)$ is the quantity with which the optical and energy-loss experiments can be described.[18] For the purpose of studying local field effects the size of the dielectric matrix $\epsilon_{\mathbf{K},\mathbf{K}'}(\mathbf{q},\omega)$ in the inversion needs to be varied. This has been done for the case of NaCl, where we have calculated the static dielectric constant ($\omega = 0$) for various $\mathbf{q}$, and for LiF where the effect of the local fields on the energy-loss spectrum has been calculated. First we will consider NaCl and use three sets of reciprocal lattice vectors for which the dielectric matrix is evaluated. The sets A, B, and C consist of reciprocal lattice vectors $\mathbf{K} = i\mathbf{a}^* + j\mathbf{b}^* + k\mathbf{c}^*$ where i, j, and k, respectively, obey the conditions $|i|$, $|j|$, $|k| \leq 0$, 1, or 2 and $\mathbf{a}^*$, $\mathbf{b}^*$, and $\mathbf{c}^*$ are the primitive reciprocal lattice vectors. Table V shows the results for a number of wave vectors $\mathbf{q}$. The

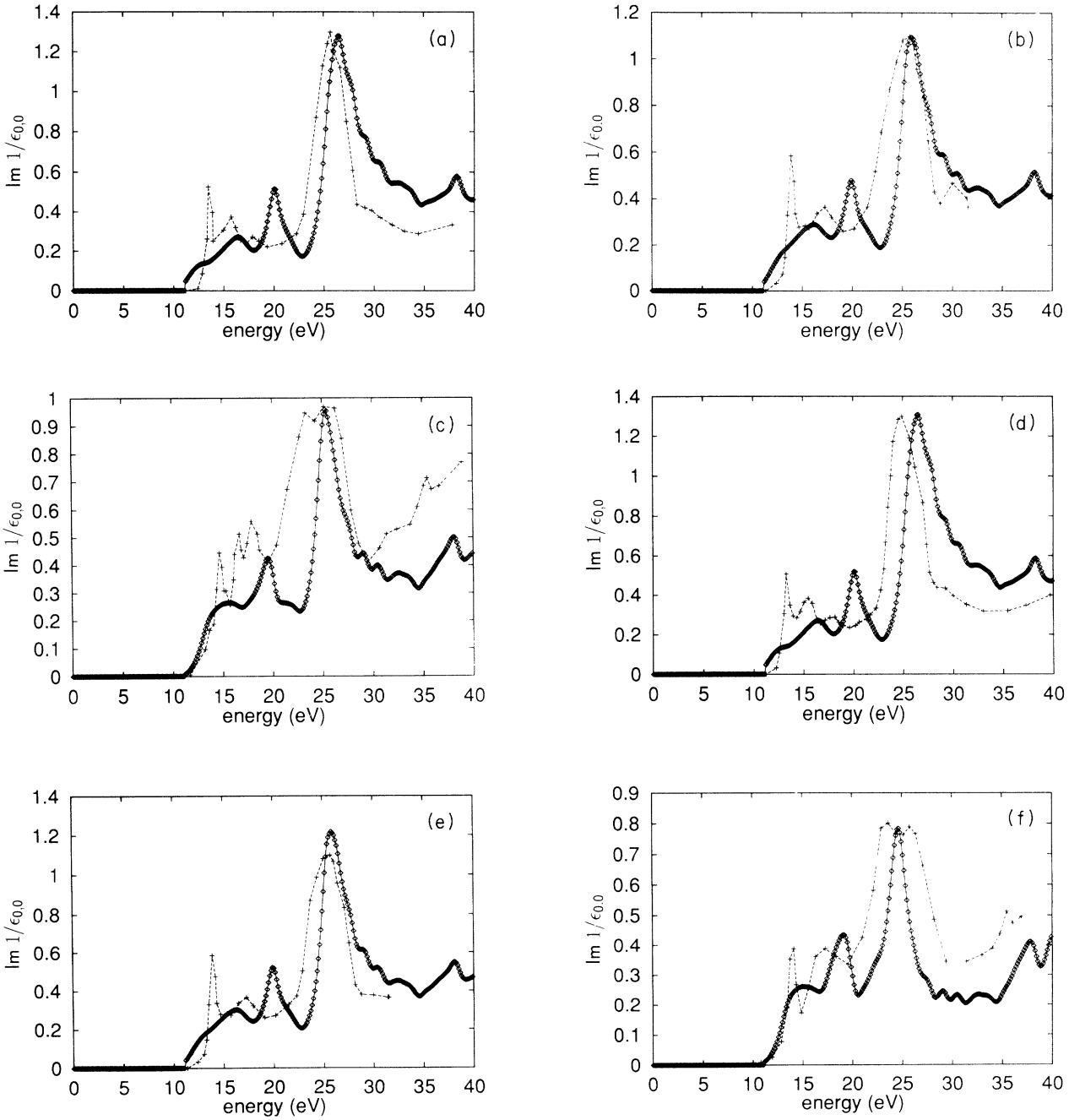

FIG. 3. Comparison of electron-energy-loss spectra of LiF (Ref. 17) and $\mathrm{Im}1/\epsilon_{0,0}(\mathbf{q},\omega)$ for various wave vectors. (a) $\mathbf{q}\|(100)$, $q = 0.23$ a.u.$^{-1}$, (b) $\mathbf{q}\|(100)$, $q = 0.68$ a.u.$^{-1}$, (c) $\mathbf{q}\|(100)$, $q = 1.51$ a.u.$^{-1}$, (d) $\mathbf{q}\|(110)$, $q = 0.23$ a.u.$^{-1}$, (e) $\mathbf{q}\|(110)$, $q = 0.68$ a.u.$^{-1}$, and (f) $\mathbf{q}\|(110)$, $q = 1.56$ a.u.$^{-1}$. The experimental spectra are indicated by crosses.

TABLE V. Effect of local fields on the macroscopic dielectric function for NaCl for various wave vectors. Local fields are included by using sets B and C of reciprocal lattice vectors in the calculation. See also text. The magnitude of wave vector $\mathbf{q}$ is given in a.u.$^{-1}$

$\mathbf{q}$	$\epsilon_M(\omega=0)$ no local fields	$\epsilon_M(\omega=0)$ with local fields B	$\epsilon_M(\omega=0)$ with local fields C
0.100, $\parallel$ (100)	2.501	2.400	2.389
1.070, $\parallel$ ($\bar{1}\bar{1}\bar{1}$)	1.591	1.481	-
0.964, $\parallel$ ($\bar{1}0\bar{1}$)	1.294	1.281	-
1.920, $\parallel$ ($0\bar{1}1$)	1.029	1.022	-
2.255, $\parallel$ ($\bar{1}\bar{1}\bar{1}$)	1.019	1.012	-
2.455, $\parallel$ (111)	1.006	1.006	-

introduction of local fields reduces the value of $\epsilon_M(\mathbf{q},\omega)$ and for low values of q this reduction is significantly larger (2–10%). For $q > 2$ a.u.$^{-1}$ the contribution of the local fields to $\epsilon_M(\mathbf{q},\omega)$ can be neglected. Similar results have been obtained by Hybertsen and Louie[1] in their calculation of the macroscopic dielectric function for various semiconductors.

Although these results indicate that local fields are important in a quantitative treatment of dielectric response, the number of off-diagonal elements that need to be taken into account can be rather small. Table V shows that for $q = 0.10$ a.u.$^{-1}$ set B, which has 27 reciprocal lattice vectors, includes most of the local field effects. Using the larger set C (125 reciprocal lattice vectors) only produces a small improvement of the dielectric constant (0.5%). Finally we will consider the contribution of local fields in (14) to the energy-loss spectra of LiF. Some information on this can already be inferred from the experimental spectra, which are not very sensitive to changes in $\mathbf{q}$ orientation in the energy range of 0–40 eV. Therefore we expect that the local fields have their main contribution in changing the spectral intensity and not in changing the peak positions, as has already been shown in the case of Si.[20,21] Our model calculations, in which set B of reciprocal lattice vectors is used, confirm this, as can be seen in Fig. 4 where both spectra (local fields included/not included) are given.

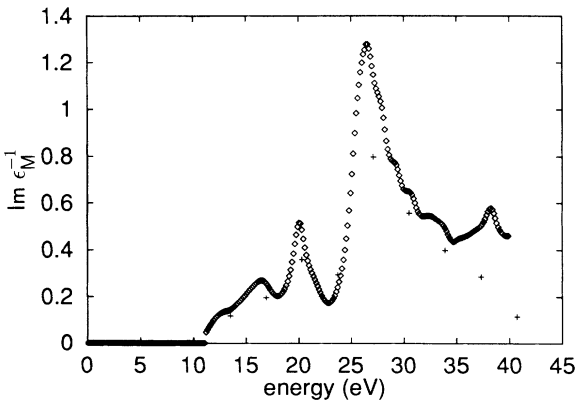

FIG. 4. Effect of local fields on $\mathrm{Im}\epsilon_M^{-1}(\mathbf{q},\omega)$ for LiF for $\mathbf{q}\parallel(100)$, $q = 0.10$ a.u.$^{-1}$. Local fields are included by using set B of reciprocal lattice vectors in the calculation. See text. The results of the local field calculation are indicated by crosses.

IV. CONCLUDING REMARKS

We have shown that if we make some well-founded assumptions about the spatial variation of the valence and conduction band wave functions and the band structure it is possible to produce a simple and fairly accurate frequency- and wave-vector-dependent model dielectric function. The present approach is based on the RPA formalism. The static dielectric matrices that are calculated within the model can be fitted to *ab initio* results, using only one parameter: the extent of the valence wave function. Moreover, the effects of local fields on the macroscopic dielectric function, which were found in *ab initio* calculations, are reproduced and sum rule requirements are obeyed. In addition, the frequency dependence of (the inverse of) the macroscopic dielectric function can be obtained from this model, and for LiF we have made a comparison between this quantity and experimental EELS spectra, giving good agreement.

ACKNOWLEDGMENTS

We are grateful for stimulating discussions and correspondence with F. Aryasetiawan, R. A. de Groot, and M. van Buuren. This work has been supported in part by the Stichting voor Fundamenteel Onderzoek der Materie (FOM) with financial support from the Nederlandse Stichting voor Wetenschappelijk Onderzoek (NWO), the Netherlands, and by the European Community programme Human Capital & Mobility (Contract No. CHRX-CT93-0337).

APPENDIX A

The evaluation of integrals of the type $\int d^3r p_\mu(\mathbf{r}) e^{i\mathbf{Q}\cdot\mathbf{r}}$ and $\int d^3r p_\mu^2(\mathbf{r}) e^{i\mathbf{Q}\cdot\mathbf{r}}$ is sketched briefly in this section. The input for these integrals is the $2p$ functions already given in the theory section [see, for example, (5)]. The axis system is rotated in order to put $\mathbf{Q}$ parallel to the z axis. The wave functions are transformed to a particular linear combination of the $2p_x$, $2p_y$, and $2p_z$ functions [these functions form an irreducible representation in SO(3)]. The resulting e^{iQz} factor can be expanded into spherical Bessel functions,

$$e^{iQz} = \sum_{l=0}^{\infty}(2l+1)i^l j_l(Qr)P_l(\cos\theta_r) \ . \tag{A1}$$

Using the orthogonality relation for the Legendre polynomials, it is a straightforward task to evaluate the integrals. We will give only the result of the calculation:

$$\int d^3r p_\mu(\mathbf{r})e^{i\mathbf{Q}\cdot\mathbf{r}} = 32\sqrt{\pi}i\cos\theta_r \sum_\nu c_\nu(\lambda_\nu)^{\frac{7}{2}} \frac{Q}{(\lambda_p^2+Q^2)^3} \ , \tag{A2}$$

$$\int d^3r p_\mu^2(\mathbf{r})e^{i\mathbf{Q}\cdot\mathbf{r}} = \sum_{\nu,\tau} c_\nu c_\tau(\lambda_\nu\lambda_\tau)^{\frac{7}{2}}\left\{\cos^2\theta_r \frac{32(\lambda_\nu+\lambda_\tau)[(\lambda_\nu+\lambda_\tau)^2-20Q^2]}{[(\lambda_\nu+\lambda_\tau)^2+Q^2]^4} + \sin^2\theta_r \frac{272(\lambda_\nu+\lambda_\tau)[Q^2+\frac{32}{272}(\lambda_\nu+\lambda_\tau)^2]}{[(\lambda_\nu+\lambda_\tau)^2+Q^2]^4}\right\} , \tag{A3}$$

where $\theta_r \equiv \theta(\hat{\mathbf{z}}, \mathbf{Q})$.

APPENDIX B

The angular integration in (10) can be separated into four terms and two of these involve nontrivial integrations. The first one is of the form

$$\int_0^\pi d\theta_\kappa \sin\theta_\kappa \int_0^{2\pi} d\phi_\kappa \kappa_z[\boldsymbol{\kappa}-(\mathbf{q}+\mathbf{K})]_z \frac{1}{(a-\boldsymbol{\kappa}\cdot\mathbf{c})^3} \ , \qquad a > \boldsymbol{\kappa}\cdot\mathbf{c} \ , \tag{B1}$$

where $\mathbf{c} = 2(\mathbf{q}+\mathbf{K})$.

The integral can be put into a more convenient form by rotating $\mathbf{c}$ parallel to the z axis and the quantization axis $\mathbf{j}$ of the p function into the xz plane. Moreover, it can be shown that

$$\frac{1}{(a-\boldsymbol{\kappa}\cdot\mathbf{c})^3} = \sum_{r=0}^{\infty}\binom{r+2}{2}\frac{(\boldsymbol{\kappa}\cdot\mathbf{c})^r}{a^{r+3}} \ . \tag{B2}$$

Including this into (B1) the integral can be reduced to a standard integral

$$\sum_{r=0}^{\infty}\binom{r+2}{2}\frac{\kappa^r c^r}{a^{r+3}}\int_0^\pi d\theta_\kappa \int_0^{2\pi} d\phi_\kappa \left\{\kappa^2 j_x^2\cos^2\phi_\kappa\cos^r\theta_\kappa\sin^3\theta_\kappa + j_z^2\left[\kappa^2\sin\theta_\kappa\cos^{r+2}\theta_\kappa - \frac{\kappa c}{2}\sin\theta_\kappa\cos^{r+1}\theta_\kappa\right]\right\} . \tag{B3}$$

The second integral is of the form

$$\int_0^\pi d\theta_\kappa \sin\theta_\kappa \int_0^{2\pi} d\phi_\kappa [\boldsymbol{\kappa}-(\mathbf{q}+\mathbf{K})]_z[\boldsymbol{\kappa}-(\mathbf{q}+\mathbf{K}')]_z \frac{1}{(a-\boldsymbol{\kappa}\cdot\mathbf{c})^3}\frac{1}{(b-\boldsymbol{\kappa}\cdot\mathbf{d})^3} \ , \tag{B4}$$

where $\mathbf{c} = 2(\mathbf{q}+\mathbf{K})$ and $\mathbf{d} = 2(\mathbf{q}+\mathbf{K}')$ and where $a > \boldsymbol{\kappa}\cdot\mathbf{c}$ and $b > \boldsymbol{\kappa}\cdot\mathbf{d}$. Also here the integral can be written in a more convenient form by rotating the axis system. In this case $\mathbf{c}$ is put parallel to the z axis and $\mathbf{d}$ is put in the xz plane. In addition both $\frac{1}{(a-\boldsymbol{\kappa}\cdot\mathbf{c})^3}$ and $\frac{1}{(b-\boldsymbol{\kappa}\cdot\mathbf{d})^3}$ are expanded as in (B2). This results in the following expansion:

$$\sum_{r,q=0}^{\infty}\binom{r+2}{2}\binom{q+2}{2}\left(\frac{c^r}{a^{r+3}}\right)\left(\frac{d^q}{b^{q+3}}\right)\kappa^{r+q}\int_0^\pi d\theta_\kappa\sin\theta_\kappa\int_0^{2\pi}d\phi_\kappa \times\{\kappa_{\mathbf{j}}^2 - \kappa_{\mathbf{j}}[(\mathbf{q}+\mathbf{K})_{\mathbf{j}}+(\mathbf{q}+\mathbf{K}')_{\mathbf{j}}] + (\mathbf{q}+\mathbf{K})_{\mathbf{j}}(\mathbf{q}+\mathbf{K}')_{\mathbf{j}}\}\cos^r\theta_\kappa\cos^q(\boldsymbol{\kappa},\mathbf{d}) \ . \tag{B5}$$

From the solution of spherical triangles it is possible to express the $\cos(\boldsymbol{\kappa},\mathbf{d})$ in terms of $\cos\theta_\kappa$, $\sin\theta_\kappa$, and $\cos\phi_\kappa$ functions:

$$\cos(\boldsymbol{\kappa},\mathbf{d}) = \cos\theta_\kappa\cos(\hat{\mathbf{z}},\mathbf{d}) + \sin\theta_\kappa\cos\phi_\kappa\sin(\hat{\mathbf{z}},\mathbf{d}) \ . \tag{B6}$$

Introducing this into (B5) the integral of (B4) can be expressed in terms of standard integrals.

[1] M. S. Hybertsen and S. G. Louie, Phys. Rev. B **35**, 5585 (1987).
[2] L. Hedin and S. Lundqvist, Solid State Phys. **23**, 1 (1969).
[3] F. Aryasetiawan, Phys. Rev. B **46**, 13 051 (1992).
[4] M. S. Hybertsen and S. G. Louie, Phys. Rev. B **34**, 5390 (1986).
[5] D. L. Johnson, Phys. Rev. B **9**, 4475 (1974).
[6] M. Ortuno and J. C. Inkson, J. Phys. C **12**, 1065 (1979).
[7] W. Hanke and L. Sham, Phys. Rev. Lett. **33**, 582 (1974).
[8] J. C. Inkson and R. D. Turner, J. Phys. C **9**, 3583 (1976).
[9] J. L. Fry, Phys. Rev. **179**, 892 (1969).
[10] G. A. Rezvani and R. J. Friauf, Phys. Rev. B **47**, 9215 (1993).
[11] S. L. Adler, Phys. Rev. **126**, 413 (1962).
[12] A. Zunger and A. J. Freeman, Phys. Rev. B **16**, 2901 (1977).
[13] E. Clementi, IBM J. Res. Dev. **9**, 2 (1965).
[14] V. Heine, Solid State Phys. **24**, 1 (1970).
[15] A. Baldereschi and E. Tosatti, Phys. Rev. B **17**, 4710 (1978).
[16] M. T. Czyżyk, R. A. de Groot, G. Dalba, P. Fornasini, A. Kisiel, F. Rocca, and E. Burattini, Phys. Rev. B **39**, 9831 (1989).
[17] J. R. Fields, P. C. Gibbons, and S. E. Schnatterly, Phys. Rev. Lett. **38**, 430 (1977).
[18] J. Fink, in *Unoccupied Electronic States*, edited by J. C. Fuggle and J. E. Inglesfield (Springer-Verlag, Berlin, 1992), p. 203.
[19] F. J. Himpsel, L. J. Terminello, D. A. Lapiano-Smith, E. A. Eklund, and J. J. Barton, Phys. Rev. Lett. **24**, 3611 (1992).
[20] S. G. Louie, J. R. Chelikowsky, and M. L. Cohen, Phys. Rev. Lett. **34**, 155 (1975).
[21] K. Sturm, Phys. Rev. Lett. **40**, 1599 (1978).